This is a peer-reviewed, accepted author manuscript of the following article:
Javadi, Y. (2015). Investigation of clamping effect on the welding residual stress and deformation of monel plates by using the ultrasonic stress measurement and finite element method.
Journal of Pressure Vessel Technology, Transactions of the ASME, 137(1), [011501].
https://doi.org/10.1115/1.4027514

Investigation of clamping effect on the welding residual stress and deformation of Monel plates by using the ultrasonic stress measurement and finite element method

Yashar Javadi [1*]

[1] Department of Mechanical Engineering, Semnan Branch, Islamic Azad University, Km. 5 of Semnan-Damghan Road, Semnan, Iran.
([*] Corresponding author's e-mail: yasharejavadi@yahoo.com; Tel: +98 9124402303, Fax: +98 231 335 4030.)

Abstract

Welding of nickel-based alloys is increasingly used in the industry to manufacture many important components of the marine industries, chemical processing, etc. In this study, a 3D thermo-mechanical finite element analysis is employed to evaluate residual stresses and deformations caused by the tungsten inert gas (TIG) welding of Monel 400 (Nickel-Copper alloy) plates. The finite element (FE) results related to the residual stresses and deformations have been verified by using the hole-drilling stress measurement and common dimensional measurement tools, respectively. Residual stresses analyzed by the FE simulation are then compared with those obtained from ultrasonic stress measurement. The ultrasonic stress measurement is based on acoustoelasticity law, which presents the relation between the acoustic waves and the stress of material. The ultrasonic stress measurement is carried out by using longitudinal critically refracted (L_{CR}) waves which are longitudinal ultrasonic waves propagated parallel to the surface inside the tested material. Two welded plates are experimentally prepared (with and without using clamp) to investigate the clamping effect on the welding residual stress

and deformations. By utilizing the FE analysis along with the L_{CR} method, the distribution of longitudinal residual stress could be achieved. It has been concluded that the applied methodologies are enough accurate to distinguish the clamping effect on the welding residual stresses and deformations of Monel plates.

Keywords: Monel; Nickel Alloy Welding; Finite Element Welding Simulation; Ultrasonic Stress Measurement; Welding Residual Stress; Welding Deformation.

1- INTRODUCTION

1.1. Monel welding process

Monel is a trademark for a series of nickel alloys, composed of nickel (up to 67%) and copper, with some iron and other trace elements (Table 1). MONEL alloy 400 is a solid-solution alloy that can be hardened only by cold working. It has considerable strength and toughness over a wide temperature range and exceptional resistance to many corrosive environments [1]. Monel 400 is widely used in many industries, especially marine and chemical processing. Some of common applications include valves and pumps, marine fixtures and fasteners, springs, chemical processing equipment, gasoline and fresh water tanks, crude petroleum stills, process vessels and piping, boiler feed-water heaters and deaerating heaters [1].

Table 1. Chemical composition of Monel 400 used in this study

Element	Ni	Cu	C	Si	Mn	S	Fe
Chemical Composition (wt %)	63.39	33.29	0.29	0.47	0.039	0.017	2.26

Conventional welding processes can be used to produce high-quality joints in nickel alloys. However, some of the characteristics of nickel alloys necessitate employing somewhat different

techniques than those used for commonly encountered materials such as carbon and stainless steels [1]. Welding procedures for nickel alloys are comparable to those used for austenitic stainless steel. In this study, Monel plates are joined by employing tungsten inert gas (TIG) welding process, which is widely used for nickel alloys joining.

1.2. Welding residual stress and deformations

Residual stresses are defined as remaining stresses inside the material after manufacturing process, in the absence of any external loads or thermal gradients. The engineering properties of industrial equipment particularly fatigue life, dimensional stability, corrosion resistance, and brittle fracture can be considerably influenced by residual stresses. Welding processes, as essential production processes in the industry, produces residual stresses at a significant level. In the presence of geometric constraints, the welding residual stresses and deformations are results of non-uniform thermal expansions and solidifications caused by the welding processes.

The welding residual stresses and deformations can be undesirable in various industrial cases related to the Monel joining. However, studies on the stress analysis of such weldments are scantly found in the literatures. Yegaie et al. [2] investigated the welding residual stresses of Monel 400 plates. They utilized finite element (FE) simulation of welding process to evaluate the residual stresses while the hole-drilling method was employed to validate the FE model. Korsunsky and James [3] evaluated welding residual stress of the nickel alloys by using a high-energy synchrotron X-ray diffraction. They succeeded to measure residual stresses of the nickel-based alloys, nondestructively. However, the ultrasonic stress measurement (which is used in this study) is not considered in the previous studies related to the nickel-based alloy.

1.3. Three-dimension thermo-mechanical finite element analysis of the welding process

It has been more than 40 years since Ueda and Yamakawa [4] firstly described a thermal elastic plastic finite element method (FEM) to predict the welding residual stress and deformation. Under the efforts of many researchers, numerous progresses have been made in the field of computational welding mechanics [5-7], which has been an important branch in the area of welding science and technology.

The majority of studies conducted before the year 2000 simulated the welding process by assuming two-dimension (2D) FE models, which have shown serious limitations in prediction of the welding residual stresses and, particularly, various types of welding deformations. Hence, the 2D model is not considered in this study to analyze the welding deformation and residual stresses.

By improving the calculation efficiency of computers, many numerical studies have been conducted to analyze the residual stresses and deformations by employing three-dimension (3D) FE models. For example, a 3D model has been used by Sattari-far and Javadi [8] to predict the welding deformations of stainless steel pipes. They investigated influence of welding sequence on welding distortions concluding that the 3D models could accurately predict the welding deformations. Since the welding deformations are also considered in this study, hence the 3D FE model is used to simulate the welding process.

1.4. Ultrasonic stress measurement

Ultrasonic stress measurement is a nondestructive method based on the linear relation between ultrasonic wave velocity and the mechanical stress inside the material. This relation is called as acoustoelastic effect, which expresses that flight time of the ultrasonic wave changes with the stress. Crecraft [9] showed that the acoustoelastic law could be used to measure stress of

the engineering materials. He employed transverse ultrasonic wave for ultrasonic stress measurement but in modern applications of the technique, longitudinal critically refracted (L_{CR}) waves are used because of their higher sensitivity to the stress. The L_{CR} wave is a longitudinal ultrasonic wave propagated parallel to the surface. Egle and Bray [10] showed that the L_{CR} wave sensitivity to the stress is highest among the other types of ultrasonic waves. The L_{CR} waves were employed to measure bending stress in the steel plates by Bray and Tang [11]. They used two different testing frequencies (2.25 MHz and 5 MHz) of the ultrasonic probes to show that the ultrasonic waves, by changing testing frequency, are able to penetrate at different depths measuring sub-surface stresses. Similarly, Javadi et al. [12] employed the ultrasonic method in the stainless steel plates for sub-surface stress measurement by using four different testing frequencies. They also compared the results of ultrasonic stress measurement with those obtained from the FE welding simulation.

1.5. Goals and objectives of this study

The main goal of this study is evaluation of the welding residual stress and deformation in the Monel plates to investigate clamping effect on the residual stresses and deformations. The FE simulation of the welding process is employed to numerically analyze the welding residual stresses and deformations while the hole-drilling measurement is used to validate the FE model. Good agreement is achieved by comparing the FE simulation results with those obtained from the ultrasonic stress measurements. It means that the L_{CR} method could be successfully used in residual stress measurement of the Monel plates. It is also concluded that using clamp leads to increasing the welding residual stresses. However, by experimental measurement and also FE simulation, the considerable decreasing trend of welding deformations of clamped Monel plates is confirmed.

2- THEORETICAL BACKGROUND

2.1. L_{CR} method

Different experimental setups could be employed for residual stresses measurements by the L_{CR} waves. As a common configuration, three ultrasonic transducers operating at the same frequency are utilized. The transducers are normal probes could be selected from the contact or immersion ultrasonic probes. Javadi and Najafabadi [13] compared the residual stresses measured by using the contact transducers with those results obtained from the immersion probes. They showed that there is no considerable difference in the ultrasonic stress measured by using contact or immersion probes hence, the contact probes are employed in this study to produce the L_{CR} wave measuring the residual stresses. To produce the L_{CR} wave, the longitudinal wave is produced at the first critical angle by a transmitter (sender) transducer, and then propagates inside and parallel to the surface of tested material. Two receiver transducers assembled in different distances from the sender finally detects the wave. The reason of employing two receiver transducers is decreasing the environmental effects, like ambient temperature, on the wave velocity. More experimental details of the L_{CR} waves could be found in several previous studies like Javadi et al. [12-14] where they presented different configurations needed to measure longitudinal residual stresses of the plates, hoop and axial residual stresses of the pipes. They also showed an accurate design for the wedge, which is a united plastic piece holding the transducers, which is also used in this study. The relation between travel-time measured by the L_{CR} wave and the corresponding uniaxial stress is developed by Egle and Bray [10] to be:

$$\Delta\sigma = \frac{E}{Lt_0}(t - t_0) \quad (1)$$

In Eq. (1), $\Delta\sigma$ is stress change, E is the elastic modulus and L is the acoustoelastic coefficient (known as acoustoelastic constant) for longitudinal waves propagated in the direction of the applied stress field. The acoustoelastic constant is measured by the uniaxial tensile test carried out over the specimens extracted from the investigated material. Since the material properties for the weld zone is different from the heat-affected zone (HAZ) and also parent material (PM), hence the acoustoelastic constant is required to be measured in all the zones independently. Also, t is travel-time of the L_{CR} wave, which is experimentally measured on the tested material while t_0 is travel-time related to the stress-free sample. Measuring the acoustoelastic constant along with the weld induced change in travel-time leads to determination of the stress changes caused by the welding process.

2.2. Finite element welding simulation

Numerical analysis of the welding residual stresses and deformations needs to take account of the mechanical properties of welds. The process is also influenced by the coupling among heat transfer, microstructure evolution and thermal stresses. However, since the finite element method is inherently a continuum-level calculation, hence simulation of the microstructural evolution is considered through simulating the material properties changes at expected transformation times and temperature. From the thermo-mechanical point of view, the heat input can be assumed as a volumetric or surface energy distribution. The fluid flow effect, which leads to homogenizing the temperature in the molten area, can be taken into account by increasing the thermal conductivity over the melting temperature. Heat transfers in solids are described by the heat equation as following:

$$\rho \frac{dH}{dt} - div(k\nabla T) - Q = 0 \quad (2)$$

$$k\nabla T.n = q(T,t) \quad \text{on} \quad \partial\Omega_q \quad (3)$$

$$T = T_p(t) \quad \text{on} \quad \partial\Omega_t \quad (4)$$

In Eq. (2-4), ρ, k, H, Q and T are density, thermal conductivity, enthalpy, internal heat source and temperature respectively. In Eq. (3), n is the outward normal vector of domain $\partial\Omega$ and q is the heat flux density that could rely on temperature and time to model convective heat exchanges on the surface; and T_p is a prescribed temperature.

The heat input is represented by an internal heat source. In this study, the double ellipsoid heat source pattern presented by Goldak and Akhlaghi [6] is employed to simulate the heat source in the FE model. The double ellipsoid model, also known as the Goldak model, is a popular model employing two ellipsoid heat source patterns to simulate how the heating energy of the welding torch is transferred to the nodes of the FE model. The moving heat source is modelled by a user subroutine in the ANSYS commercial software.

Material modeling has always been a complicated stage in the welding simulation because of material data is lacking at elevated temperatures. Some simplifications and approximations are normally employed to overcome this problem. These simplifications are necessary due to both lack of data and numerical difficulties when trying to model the actual high-temperature properties of the material. The elevated temperature properties of Monel 400, shown in Fig.1, are extracted from Yegaie et al. [2].

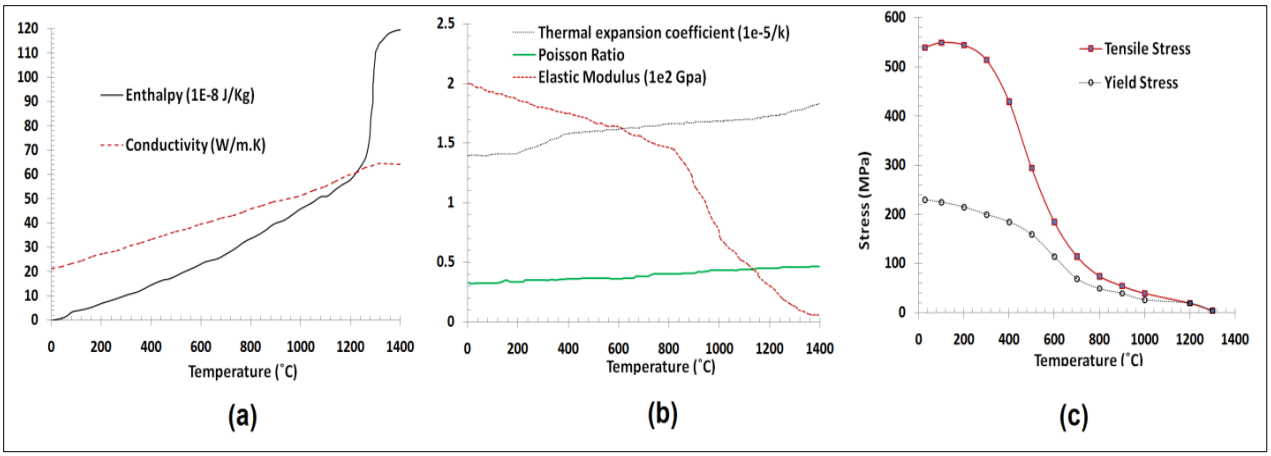

Fig.1. Thermal and mechanical material properties of Monel 400 (extracted from Yegaie et al. [2])

The FE problem is formulated as a successively coupled thermo-mechanical analysis. First, a nonlinear thermal analysis is performed to find the temperature history of the entire domain. Then, the results of thermal analysis are applied as thermal body loads in a nonlinear mechanical analysis, which determines residual stress and deformations. The mesh geometry and dimension of the FE model is the same for both thermal and mechanical analysis. The general-purposed FE program ANSYS is used for the analysis. A full Newton-Raphson iterative solution technique with direct sparse matrix solver is employed to reach the solution. During the thermal analysis, the temperature and temperature dependent material properties are quickly changed. Hence, the full Newton-Raphson technique with using modified material properties is believed to give more accurate results.

The common "Element Birth and Death" technique is used to model the deposited weld [6]. A complete FE model is generated in the start of the analysis while all elements representing the deposited weld (except elements for the tack welds) are deactivated by assigning them a very low stiffness. During the thermal analysis, all the nodes of deactivated elements (excluding those shared with the base metal) are fixed at the room temperature till the birth of the corresponding

elements. Deactivated elements are reactivated sequentially when the welding torch arrives over them.

The mesh size is optimized according to the accuracy of FE results while the meshing model is shown in Fig. 2. The final selected model is model No. 4 which is compared with 5 other models (Table 2) while the comparison criterions are calculation time and accuracy of the residual stresses analyzed by the FE model. Hence, six FE models with different meshing size are run and the residual stress results are compared with those obtained from the hole-drilling measurement (Fig. 3). The symmetry about the weld line is assumed in all the models, which simulate three weld passes. Selecting the most effective mesh size leads to the accurate results along with less time-consuming calculations. Furthermore, a sort of calibration is considered in the FE modeling of the welding process. Since the exact measurement for some of the welding parameters, e.g. welding efficiency, is not practical hence these parameters are varied in the FE simulation to reach the maximum of agreement between the FE results with those obtained from the hole-drilling measurement.

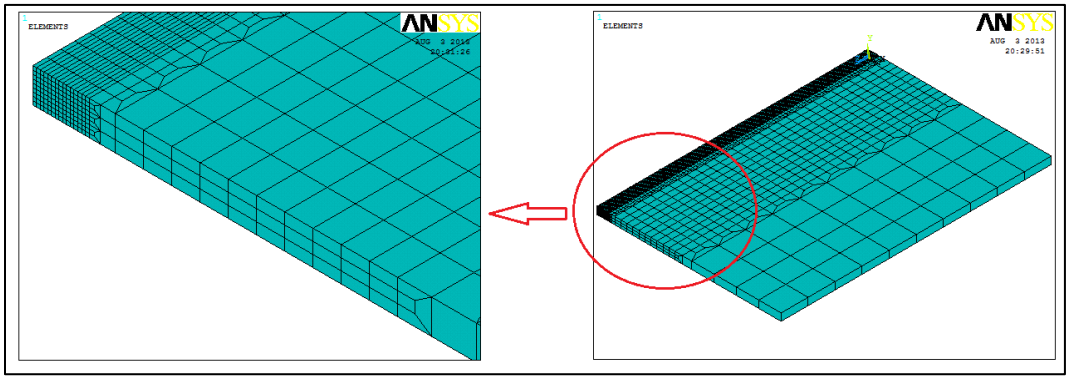

Fig.2. FE model selected in this study (Model No. 4)

Table 2. Details of six FE models compared to optimize mesh size

Model No.	Number of the Elements in the Weld Line	Number of the Elements	Mesh Dimensions in the Weld Zone (mm)	Number of the Nodes	Calculation Time (hour)
1	22	690	3.33 × 5 × 10	1012	3
2	44	1350	1.1 × 1.3 × 5	1980	6
3	44	6686	1 × 0.67 × 5	10402	21
4	90	14859	1 × 0.67 × 2.44	22432	84
5	135	22204	1 × 0.67 × 1.63	33542	174
6	225	36894	1 × 0.67 × 0.98	55753	495

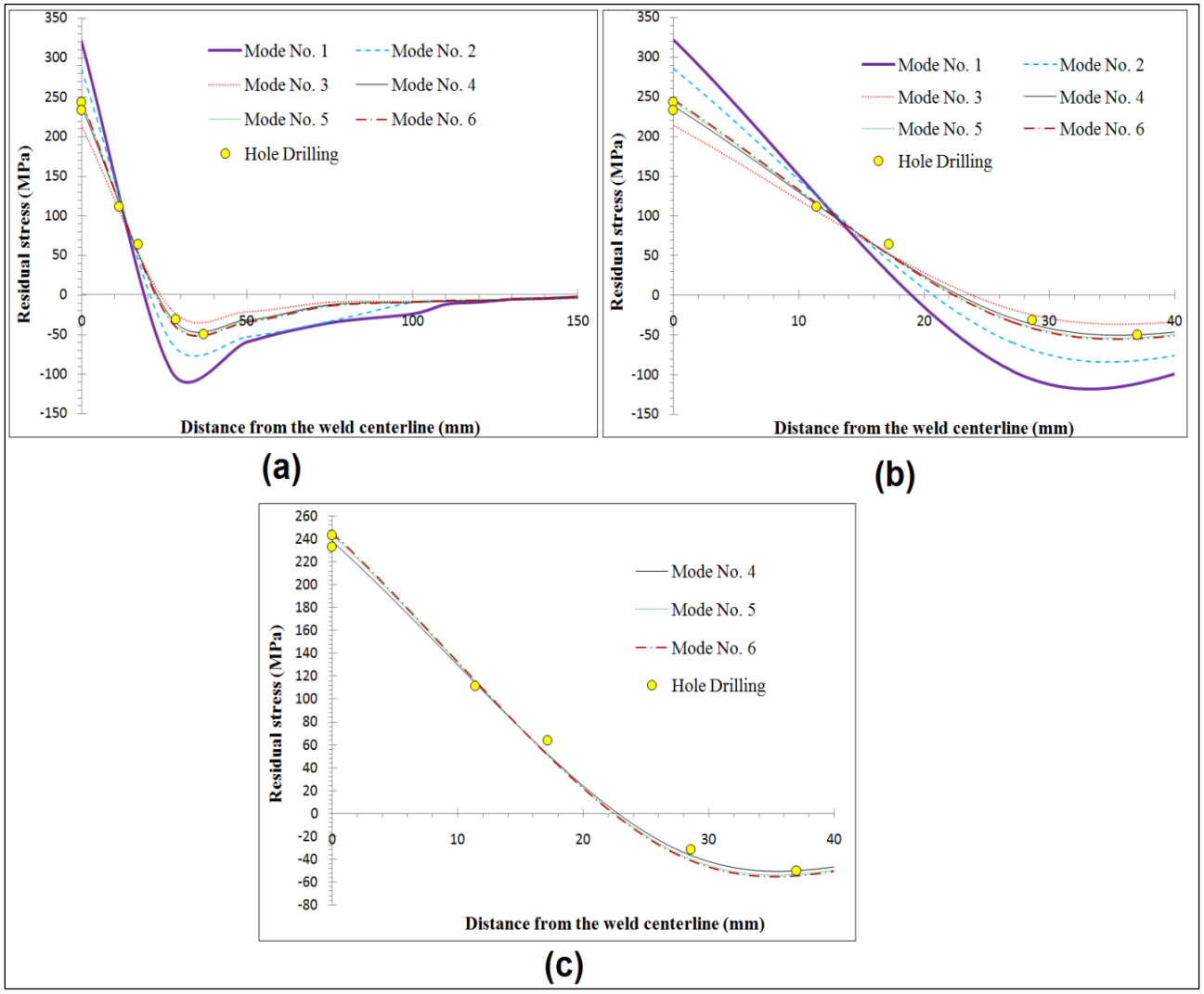

Fig. 3. The residual stresses analyzed by different six FE models (Model No. 1-6: a and b; Model No. 4-6: c) and comparison with hole-drilling results

According to the results shown in Fig. 3-a and Fig. 3-b, residual stress analyzed by using the FE model No. 1-3 leads to non-accurate results while the results of model No. 4-6 have good agreement with residual stresses measured by the hole-drilling method. Hence, the results of model No. 4-6 are compared again in Fig. 3-c which shows approximately same results obtained from these three models. However, according to the Table 2, the calculation time of model No. 4,5 and 6 is equal to 84, 174 and 495 hours respectively while there is no considerable difference in the accuracy of these models. The model No. 4 could analyze the residual stresses with enough accuracy along with a reasonable calculation time hence; this model is considered as the final result of mesh optimization process.

3- EXPERIMENTAL PROCEDURES

3.1. Sample Description

In this study, the plates from Monel® 400 (UNS N04400/W.Nr. 2.4360 and 2.4361) are welded to investigate the welding residual stresses and deformations. Two 220×150×6 mm plates are welded in V-groove (90° included angle) by employing tungsten inert gas (TIG) welding process. Multi-pass butt-weld joint geometry is used while the welding procedure specifications (WPS) are listed in Table 3. The plates are tacked weld in two points while clamping is used during the welding process of Plate 2 (no clamp is used for Plate 1). It is not practical to test non-flat surfaces in the ultrasonic stress measurement hence; the weld reinforcement is removed by employing a 30000-rpm hand grinder machine. A water-cooling system is employed to control the grinding temperature and prevent producing new thermal stresses.

Table 3. WPS for Monel welding process

Sample	Pass No.	Ampere (A)	Voltage (V)	Travel Speed (mm/sec)	Clamping	Other Specifications
Plate 1	1	100	20	3.6	No	Groove Angle: 90˚; Root Gap: 1.5 mm; Root Opening: 1.5 mm. Filler metal material: Monel Filler Metal 60 (AWS A5.141_ER NiCu-7); Filler metal diameter: 2.4 mm. Welding Process: TIG welding; Gas: Argon (10 lit/min);. Surface cleaning: Hot water with soap; Surface oxide removing: Grinding 5 cm distance from the weld; Interpass cleaning: Stainless steel brushing. Tack weld: Two tacks on the corners.
	2	110	20	1.8		
	3	120	20	1.4		
Plate 2	1	100	20	3.7	Yes	
	2	110	20	1.7		
	3	120	20	1.5		

3.2. Measurement Devices

3.2.1. Ultrasonic stress measurement

The most important step in ultrasonic stress measurement is measuring time of flight (TOF) related to the L_{CR} wave. The TOF measurement devices, shown in Fig. 4, include an ultrasonic portable box, laptop and ultrasonic transducers. A moving mechanical table is also used to move the transducers over the investigated plates with proper accuracy and stability. The ultrasonic portable box is equipped with an analogue to digital (A/D) converter which is controlled by synchronization between the pulser signal and the internal clock. The internal clock works with the resolution of 1 ns allowing precise TOF measurement. Three normal ultrasonic transducers are assembled in an integrated wedge to measure TOF related to the L_{CR} wave propagated in the investigated material. The wedge material is poly methyl methacrylate (PMMA), under the trademark Plexiglas, which is constructed by the laser cutting and CNC machining. The ultrasonic wave is produced at the first critical angle by the transmitter transducer, passing from the wedge and then propagates as the L_{CR} wave inside the material. Based on the Snell's law, the

first critical angle related to the ultrasonic wave passing from the plexiglas wedge and propagating in the Monel material is calculated equal to 31.5˚ which should be considered in machining process to construct the wedge. The L_{CR} wave is finally detected by two receiver transducers assembled in different distance from the sender while the frequency of all the transducers is equal to 2 MHz. The pressure screw supplies a constant and continuous pressure over the wedge while the pressure accuracy is controlled by employing a load cell. The pressure is needed in order to keep constant thickness of ultrasonic couplant layer between the wedge and tested plate.

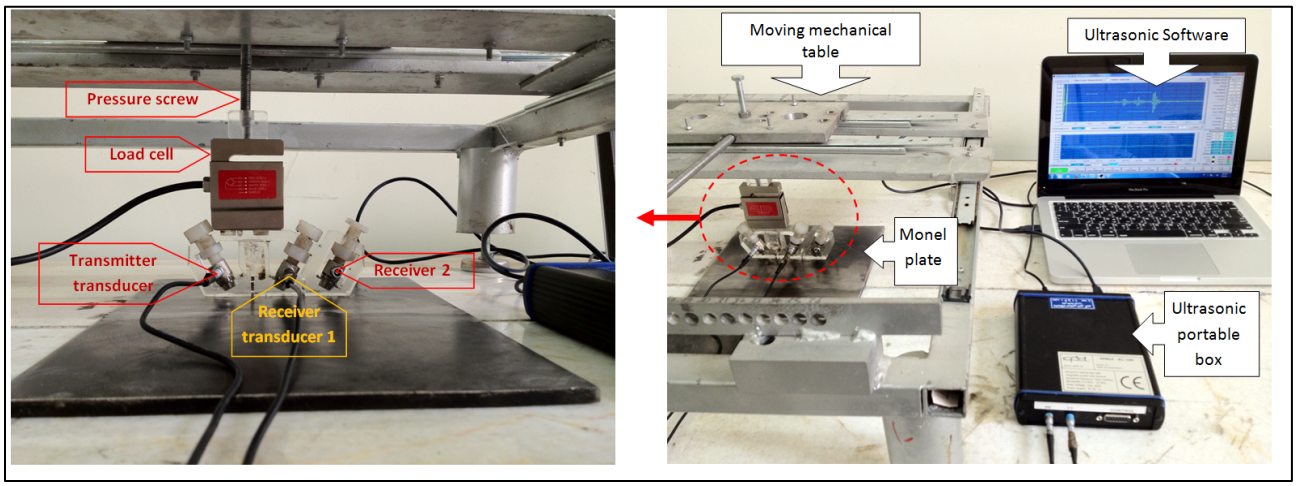

Fig.4. Ultrasonic TOF measurement devices

According to Eq. (1), the acoustoelastic constant (L) is also needed to be measured in other to evaluate the stress. The standard uniaxial tensile test is employed to evaluate the acoustoelastic constant while the tensile test specimens are extracted from the Monel plates. During the tensile test, the TOF measuring devices are employed while the transducers are assembled on the tensile test specimen in order to measure flight-time (t) of the L_{CR} wave. However, a stress-relieving heat-treatment is already required to relax the residual stresses of the tensile test specimen. By assembling the TOF measurement devices on the stress-free specimen, the t_0 is firstly achieved.

By employing a tensile test standard machine, the tensile test (σ) is increased step by step; meanwhile the flight-time (t) is measured in each step. The elastic modulus (E) could also be measured by using the tensile test results or obtaining from the material properties tables. As a result, the acoustoelastic constant (L) would be calculated based on Eq. (1).

In this study, the tensile test specimens are extracted from the weld zone and parent material (PM) to measure the E and L in each of these zones. The tensile test specimens are manufactured according to the Sheet type (0.5 in. wide) sample presented in the ASTM: E8 standard.

Finally, the acoustoelastic constant is measured equal to 1.7 and 1.96 in the PM and weld zone respectively.

3.2.2. Residual stress measurement by hole-drilling method

The residual stresses measured by the ultrasonic method will be compared with those obtained from the FE welding simulation. However, the FE results also need to be verified by another experimental measurement results which is the hole-drilling method. The hole-drilling method is carried out in six different points according to the characterizations described in ASTM: E837. This semi-destructive technique measures the strains relaxed by incremental drilling of a small hole which its diameter is equal to 1.5 mm. The strains are evaluated using a strain gauge rosette after each depth increment and the residual stresses are then calculated employing equations established by ASTM: E837.

3.2.3. Measurement of the welding deformations

The deformations are measured to compare the Plate 1 and Plate 2 in other to find the effect of using clamp on deformations produced by the welding process. The angular shrinkage (Fig. 5) is the most important deformation type which is considered in this study. It is obvious that a

considerable amount of angular shrinkage is produced in Plate 1 which was welded without using of the clamp. The angular shrinkage is accurately measured by employing a coordinate-measuring machine (CMM).

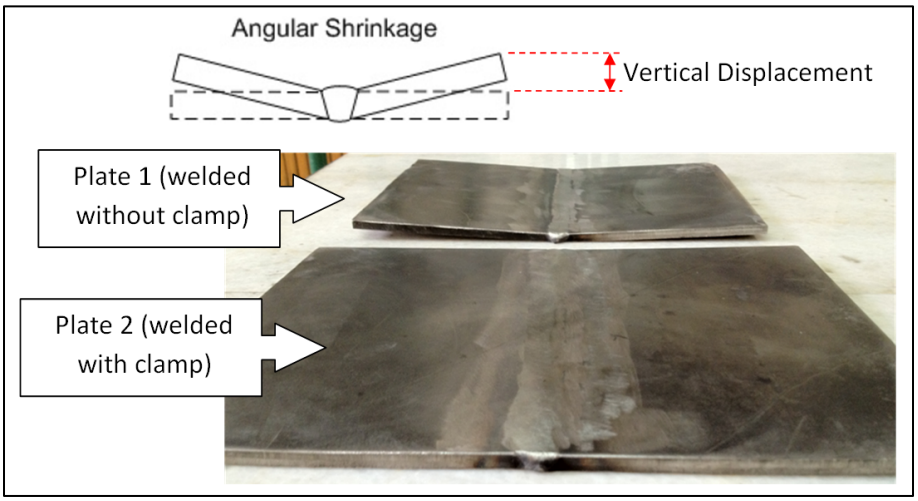

Fig.5. Angular shrinkage produced after the welding of Monel plates

4- RESULTS AND DISCUSSION

4.1. Longitudinal residual stress

The longitudinal residual stresses are analyzed by FE welding simulation, measured by ultrasonic method and verified by hole-drilling measurement. All the results, shown in Fig. 6a, are longitudinal (axial) residual stresses obtained for a plane perpendicular to the weld line of Plate 1 in Z=110 mm while the FE model is run for only one side of the plate with symmetry assumption. The results are considered as the surface stresses which are obtained in 2 mm depth from the surface. The 2 mm depth is related to the penetration depth of 2 MHz transducers producing the L_{CR} waves while the details of penetration depth measurement are reported by Javadi et al. [12]. It should be noticed that the L_{CR} ultrasonic method measures average of

stresses in the 2 mm depth hence, the average of stresses in 0-2 mm from the surface are also considered in obtaining the FE simulation results. Furthermore, the depth of hole produced during the hole-drilling measurement is equal to 2 mm hence; the average of stresses in this hole is also reported by the hole-drilling method.

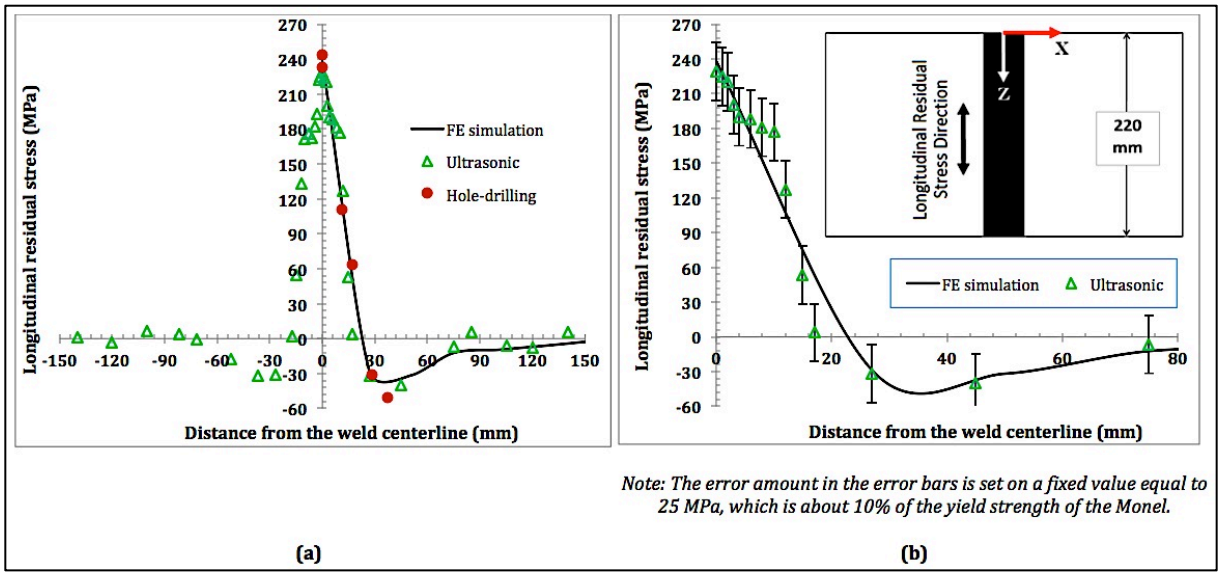

Fig.6. Longitudinal (axial) residual stress evaluated by FE, ultrasonic and hole-drilling method (Plate 1; in Z=110 mm)

The FE simulation results have good agreement with residual stresses measured by the hole-drilling method hence, the FE model has enough accuracy to be used as the verification of the ultrasonic measurements. From Fig. 6b, for the majority of the points, the difference between the residual stresses measured by the ultrasonic method with those obtained from the FE simulation does not exceed 25 MPa, which is about 10% of the yield strength of the Monel plate. It means that the ultrasonic and FE simulation results have reasonable agreement, which is the confirmation of the L_{CR} potential in stress evaluation of Monel plates.

4.2. Deformation measurement results

The angular shrinkage of Plate 1 is measured by employing a CMM. The measurement is carried out on the surface of plate in Z=110 mm that is the middle of weld line. The results are shown in Fig. 7 which shows that the maximum of vertical displacement is produced in left corner of the plate and is equal to 7.32 mm.

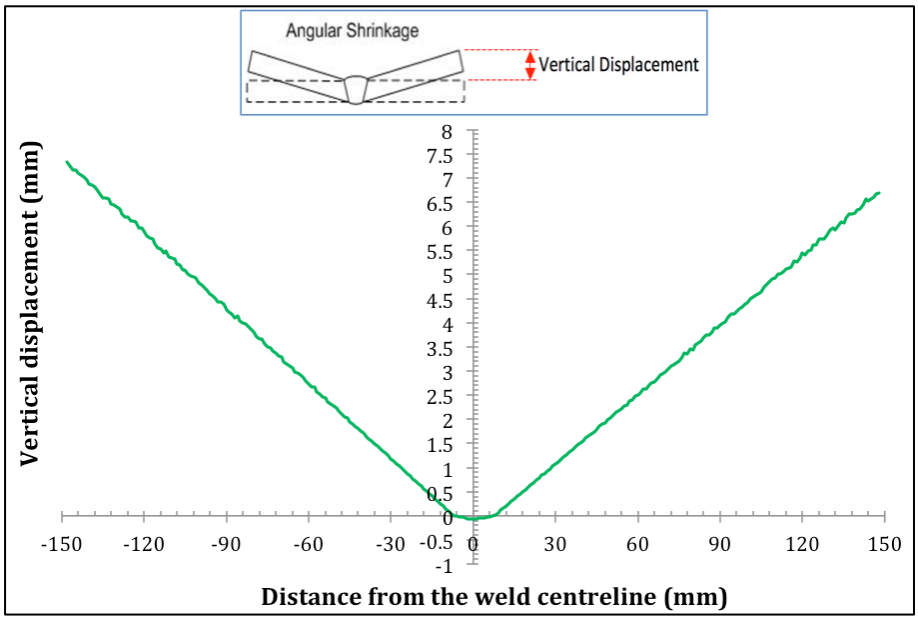

Fig.7. Angular shrinkage (Plate 1; in Z=110 mm)

4.3. Influence of using the clamp

The effect of clamping is investigated by comparing the residual stress and deformation measured on Plate 1 (no clamp) and Plate 2 (with clamp). The comparison results are shown in Fig. 8 and Fig. 9 related to the residual stress and deformations respectively. It is shown that using clamp during the TIG welding of Monel plates leads to increasing the longitudinal residual stress along with dominate decrease in the deformations. By using clamp, the peak of longitudinal residual stress increases from 229 MPa to 253 MPa while the angular shrinkage decreases from 7.32 mm to 1.61 mm. It means that, welding Monel plates by using clamp leads

to about 10 percent increase in the residual stress however, the angular shrinkage is less than a quarter of no clamp sample. It can also be concluded that the ultrasonic stress measurement using the L_{CR} waves (which is used for comparing Plate 1&2) has enough resolution to distinguish less than 25 MPa differences in the longitudinal residual stresses caused by using the clamp.

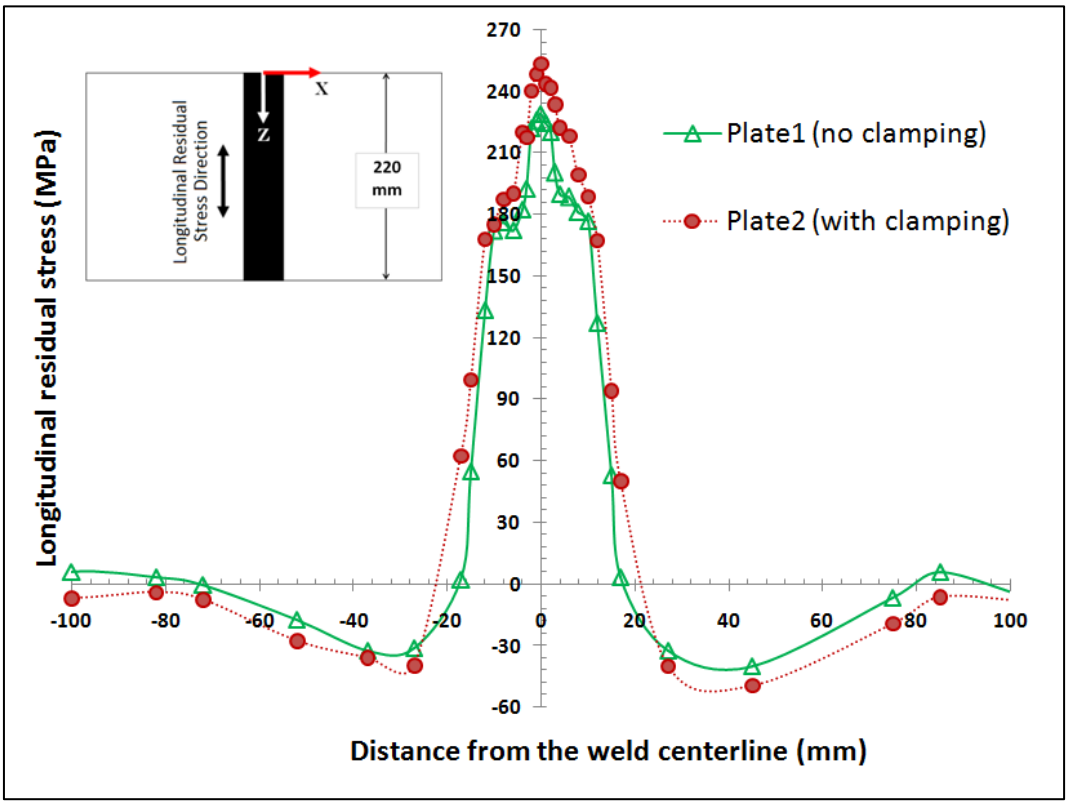

Fig.8. Clamping effect on the longitudinal residual stress (ultrasonic stress measurement in Z=110 mm)

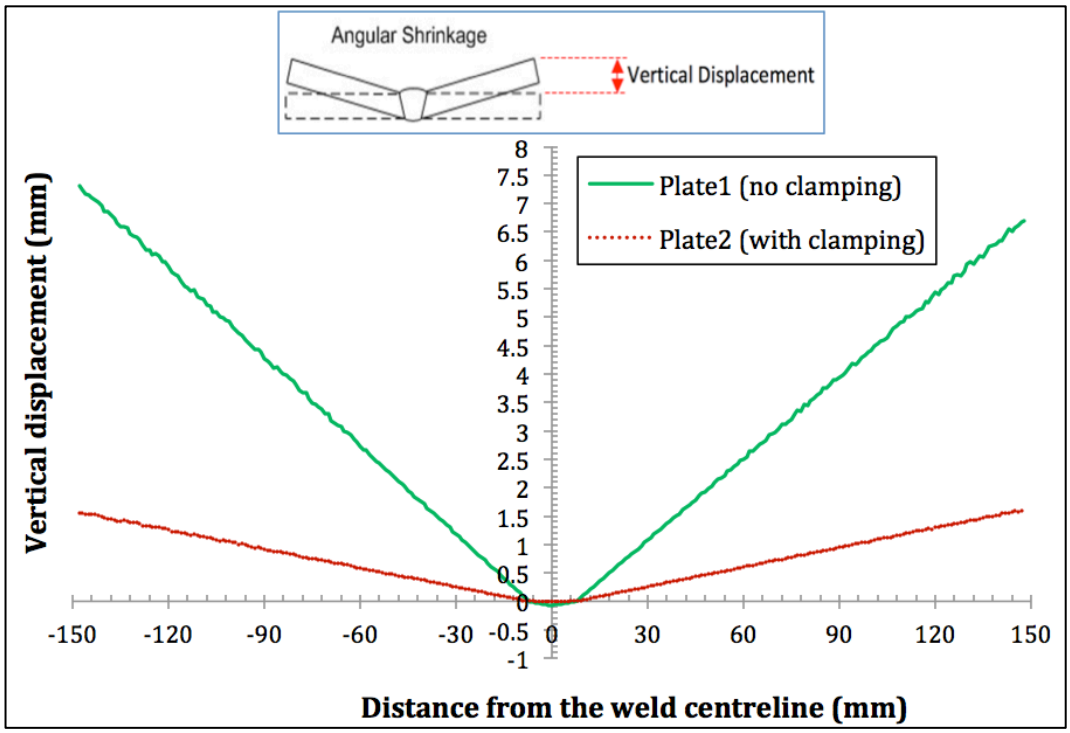

Fig.9. Clamping effect on the welding deformations

5- CONCLUSIONS

The main goal of this study is evaluation of the welding residual stress and deformation in the Monel plates to investigate the clamping effect on the residual stresses and deformations. The finite element welding simulation, the L_{CR} ultrasonic stress measurement, the hole-drilling method and the angular shrinkage measurement are employed to reach this goal. According to the achieved results, it can be concluded that:

1) The reasonable agreement achieved in comparing the FE simulation with the ultrasonic stress measurement shows that the L_{CR} ultrasonic method has good potential to be employed in residual stress measurement of Monel plates.
2) The ultrasonic stress measurement by using the L_{CR} waves shows enough accuracy to distinguish the clamping effect on the longitudinal residual stresses.

3) The welding process of Monel plates by using clamp leads to about 10 percent increase in the longitudinal residual stress.
4) The angular shrinkage of Plate 2 (welding with clamp) is less than a quarter of Plate 1 (welding without clamp).

REFERENCES

1- Special Metal Corporation (SMC), 2003, "Special metals joining," Publication Number: SMC-055, http://www.specialmetals.com

2- Yegaie, Y.S., Kermanpur, A. and Shamanian, M., 2010, "Numerical simulation and experimental investigation of temperature and residual stresses in GTAW with a heat sink process of Monel 400 plates," Journal of Materials Processing Technology, **210**, pp. 1690-1701.

3- Korsunsky, A.M. and James, K.E., 2010, "Residual Stresses Around Welds in Nickel-based Superalloys," Journal of Neutron Research, **12**, pp. 153-158.

4- Ueda, Y. and Yamakawa, T., 1972, "Thermal stress analysis of metals with temperature dependent mechanical properties," Proc. International Conference on Mechanical Behavior of Materials, S. Taira, eds., Kyoto, Japan, **3**, pp.10–20.

5- Feng, Z., 2005, Processes and Mechanisms of Welding Residual Stress and Distortion, Woodhead Publishing in Materials, Cambridge, UK.

6- Goldak, J. and Akhlaghi, M., 2005, Computational welding mechanics, Springer, New York, USA.

7- Lindgren, L.E., 2007, Computational Welding Mechanics: Thermomechanical and Microstructural Simulations, Woodhead Publishing in Welding, Cambridge, UK.

8- Sattari-Far, I. and Javadi, Y., 2008, "Influence of welding sequence on welding distortions in pipes," Int. J. of Pressure Vessels and Piping, **85**, pp. 265–274.

9- Crecraft, D.I., 1967, "The Measurement of Applied and Residual Stresses in Metals Using Ultrasonic Waves," J. Sound. Vib., **5**, pp. 173-192.

10- Egle, D.M. and Bray, D.E., 1976, "Measurement of Acoustoelastic and Third-Order Elastic Constants for Rail Steel," J. Acoust. Soc. Am., **60**, pp. 741-744.

11- Bray, D.E. and Tang, W., 2001, "Subsurface stress evaluation in steel plates and bars using the LCR ultrasonic wave," Nuclear Engineering and Design, **207**, pp. 231-240.

12- Javadi, Y., Akhlaghi, M. and Najafabadi, M.A., 2013, "Using Finite Element and Ultrasonic Method to Evaluate Welding Longitudinal Residual Stress through the Thickness in Austenitic Stainless Steel Plates," Materials and Design, **45**, pp. 628–642.

13- Javadi, Y. and Najafabadi, M.A., 2013, “Comparison between contact and immersion ultrasonic method to evaluate welding residual stresses of dissimilar joints,” Materials and Design, **47**, pp. 473–482.

14- Javadi, Y., Pirzaman, H.S., Raeisi, M.H. and Najafabadi, M.A., 2013, “Ultrasonic Evaluation of Welding Residual Stresses in Stainless Steel Pressure Vessel,” Journal of Pressure Vessel Technology, **135**, pp. 1-6.

LIST OF TABLE CAPTIONS

LIST OF FIGURE CAPTIONS